NeuroImage 54 (2011) 1151–1158

Contents lists available at ScienceDirect

NeuroImage

journal homepage: www.elsevier.com/locate/ynimg

Extended unified SEM approach for modeling event-related fMRI data

Kathleen M. Gates [a,*], Peter C.M. Molenaar [a], Frank G. Hillary [b], Semyon Slobounov [c]

[a] Department of Human Development and Family Studies, The Pennsylvania State University, University Park, PA, USA
[b] Department of Psychology, The Pennsylvania State University, University Park, PA, USA
[c] Department of Kinesiology, The Pennsylvania State University, University Park, PA, USA

ARTICLE INFO

Article history:
Received 5 April 2010
Revised 4 August 2010
Accepted 19 August 2010
Available online 15 September 2010

ABSTRACT

There has been increasing emphasis in fMRI research on the examination of how regions covary in a distributed neural network. Event-related data designs present a unique challenge to modeling how couplings among regions change in the presence of experimental manipulations. The present paper presents the extended unified SEM (euSEM), a novel approach for acquiring effective connectivity maps with event-related data. The euSEM adds to the unified SEM, which models both lagged and contemporaneous effects, by estimating the direct effects that experimental manipulations have on blood-oxygen-level dependent activity as well as the modulating effects the manipulations have on couplings among regions. Monte Carlos simulations included in this paper offer support for the model's ability to recover covariance patterns used to estimate data. Next, we apply the model to empirical data to demonstrate feasibility. Finally, the results of the empirical data are compared to those found using dynamic causal modeling. The euSEM provides a flexible approach for modeling event-related data as it may be employed in an exploratory, partially exploratory, or entirely confirmatory manner.

The introduction of functional MRI (fMRI) nearly two decades ago propagated a wealth of research examining the response to experimental stimulation in predefined brain regions of interest (ROIs). Having amassed knowledge on which distinct ROIs correspond to specific manipulations, there has been increasing emphasis in fMRI research to examine not only what regions are active, but how ROIs covary in a distributed neural network. This more recent emphasis in neural connectivity aims to discover how spatially disparate regions temporally relate in response to task demands. The driving principle supposes that brain functioning can best be understood as an integrated process involving spatially distributed regions across time (Tononi et al., 1998; Sporns et al., 2004) rather than as a response localized in only one or two highly specialized areas. Such approaches fall under the broad domain of "connectivity mapping", a set of modeling techniques that estimate the extent to which activity among previously specified ROIs' relate (Friston and Stephan, 2007). These relationships between ROIs in connectivity maps are often referred to as, "couplings" (e.g., Friston, 2007). The most prominent techniques for modeling spatial integration identify couplings among ROIs at baseline (or resting state) separately from couplings occurring when an experimental manipulation is presented. This approach works well for block designs but is difficult to implement with event-related designs. At present there remains a dearth of techniques appropriate for identifying changes in spatial integration occurring in the presence of event-related manipulations.

The present paper first offers a brief overview of relevant methods for examining "effective connectivity" networks, defined as maps which identify directional couplings among predefined ROIs (Friston and Stephan, 2007). Importantly, the present paper outlines how the majority of approaches, such as traditional structural equation models (SEM),vector autoregression (VAR) and unified SEM (uSEM), neglect to directly estimate the influence that event-related experimental manipulations has on connections, which is precisely the information of interest to researchers. We then discuss the dynamic causal model (DCM) which to date is the sole approach for including event-related manipulations and their influence on couplings among ROIs. These approaches to modeling effective connectivity (e.g., SEM, VAR, uSEM, and DCM) have advanced our understanding of distributed neural networks in the functional imaging literature. Still, there remain challenges with each of the modeling techniques to date. We offer a novel approach, the extended unified SEM (euSEM) which advances current techniques from within a general linear model framework. Specifically, the euSEM (1) models the effects on ROI activity of stimuli used in event-related experimental designs, (2) simultaneously estimates directed contemporaneous and lagged coupling parameters among ROIs, (3) estimates the modulating effect that the experimental manipulation has on couplings among ROIs, (4) may be identified using confirmatory, partially exploratory, or entirely

* Corresponding author. Department of Human Development and Family Studies, The Pennsylvania State University, S110 Henderson, University Park, PA 16802, USA.
E-mail address: kgates@psu.edu (K.M. Gates).

1053-8119/$ – see front matter © 2010 Elsevier Inc. All rights reserved.
doi:10.1016/j.neuroimage.2010.08.051

exploratory approaches based on the Lagrange multiplier test, and (5) can be applied to both group and individual data.

Current approaches for effective connectivity mapping

Effective connectivity maps, as currently employed, estimate directed couplings among ROIs that have been defined by the researcher either anatomically or by using tests of statistical significance to extract information from voxels which contain the greatest change in BOLD response. In either case, the ideal ROIs are hypothesis-driven and informed by previous experimental manipulation. Thus researchers can expect a degree of relatedness among ROIs since the selection process supposes that the chosen ROIs will increase in level in the presence of the experimental manipulation. However, it is critical to keep in mind that the general linear model employed to determine which areas are active looks for mean differences in the BOLD signal between experimental conditions. In contrast, connectivity maps are primarily concerned with the covariance in the signal between ROIs. A bulk of emerging research on resting state or default mode networks demonstrate that coordinated variations exist in the absence of experimental manipulations (Raichle and Snyder, 2007). As such, shared contemporaneous and lagged variation among ROIs may occur at times when the experimental manipulation is not presented. Along a similar rationale, shared variation in BOLD signals could occur between ROIs only in the presence of an experimental manipulation but not when the manipulation is absent, in which case the experimental manipulation is said to modulate the relationship among the ROIs. Finally, shared variation among ROIs could be similar in the presence and absence of the experimental manipulation. Connectivity maps attempting to explain relations among ROIs usually neglect to explicate in what context the couplings exist.

Structural equation modeling (SEM) is the most popular method for researchers aiming to model effective connectivity (McIntosh and Gonzalez-Lima, 1994). Allowing for directed paths, SEM simultaneously models relationships among ROIs. Two major shortcomings with this approach are that SEM assumes linearity in the relationships between ROIs and considers experimental manipulation (i.e., task related change and external input) as stochastic or undetermined rather than included as a predictor variable in the model (Friston, 2007). SEM thus works best on data where one can assume similar relations among ROIs across a block of time but becomes ill-suited for event-related designs which may provoke couplings immediately following a stimulus that differ from those existing in the absence of the stimuli (de Marco et al., 2009). Yet another limitation comes from the tradition in fMRI research of using SEM largely for confirmatory analysis. At this early phase of research designed to understand effective connectivity, exploratory approaches may complement confirmatory approaches by offering the opportunity to acquire atheoretical models of how structures within a network relate. One final limitation of the traditional SEM approach concerns the reliable finding that BOLD time series data contain serial dependencies, or "lagged effects", meaning that previous input to a voxel or region influences later signal in that voxel or region (Harrison et al., 2007). Similarly, activity occurring at a remote location at a previous time point may also influence current levels of activity at a second region. Traditional SEM employed in fMRI research does not consider these lagged effects. By neglecting the influence of lagged relations, biased estimates occur and temporal precedence (which is just one criteria necessary to establish causality) is unknown.

Approaches such as vector autoregression (VAR) and Granger causality testing address one of SEM's shortcomings by modeling lagged relationships among regions (Goebel et al., 2003). However, these approaches obtain biased estimates by not considering contemporaneous relations (Gates et al., 2010). The unified SEM (uSEM; Kim et al., 2007) has recently been presented as a remedy for this issue. The uSEM estimates contemporaneous relationships much like traditional SEM but improves upon the model by simultaneously considering lagged effects by means of VAR, thus making this approach dynamic (Kim et al., 2007). An automatic search procedure allows for the uSEM to be entirely data-driven, offering a substantial degree of flexibility when compared to alternative approaches (Gates et al., 2010). However, even with these improvements upon the traditional SEM, the model assumes that relations among ROIs are linear and continues to be inappropriate for event-related designs.

One critical remaining challenge for the SEM,VAR, and uSEM approaches is that none include an estimate of the effects of experimental manipulations on ROI activity. Experimental manipulation, such as the presentation of stimuli, carries the possibility of directly affecting ROI activity or affecting the couplings among ROIs. For instance, some ROIs may have a resting state relationship with another ROI and become deactivated with the presence of external stimuli. Conversely, couplings among ROIs identified during a task involving stimuli in a block design may be detecting covariance primarily attributable to resting state brain functioning and have little to do with the task. Friston et al. (1997) offered a preliminary solution within the general linear model framework which modeled the contemporaneous interactions between BOLD activity and experimental manipulations. However, as the errors associated with predicted ROI activity were assumed to be independently distributed, this model does not account for lagged couplings among ROIs or the lagged influence of the experimental manipulation on BOLD activity. Thus, there is a clear need for connectivity modeling that allows for different path coefficients representing the potentially distinct roles ROIs may have at the time of task stimulation.

Dynamic causal modeling (DCM) addresses the need to model event-related experimental manipulations while considering the changes in BOLD activity. Providing perhaps the most statistically sophisticated approach to date, DCM incorporates the neuronal-hemodynamic relationship into a dynamic model of BOLD activities using Bayesian estimation (Friston, 2007; Sarty, 2007). DCM estimates the modulating effects of external input on the paths between ROIs to arrive at a bilinear state-space approximation, making it unlike previously described models which assume linearity in the relations between ROIs. As DCM constitutes a system in continuous time the direct and bilinear (or modulating) effects of input establish themselves after an infinitesimal amount of time. Two characteristics of the DCM provide reason for developing alternative or complementary methods for bilinear estimation. First, DCM represents the dynamics of BOLD activities as being deterministic with the only stochastic influence being the additive measurement error. In the absence of external input, the DCM will likely estimate ROI activity to be constant. Prior research on resting state or default mode models indicate that BOLD activity fluctuates even in the absence of experimental manipulation (Raichle and Snyder, 2007). Second, the DCM is confirmatory, necessitating *a priori* specification of directed couplings between ROIs as well as all modulating effects. At this early state in connectivity research, this model could be supplemented by one which allows for error and exploratory analysis. A successful approach would offer the opportunity to model between-task couplings as well as on-task couplings among ROIs while attending to the biases introduced when not considering sequential dependencies among the BOLD data.

Extended unified SEM

The present paper presents a practical approach, the extended unified SEM (euSEM) for estimating direct and modulating external experimental influences on BOLD activity without *a priori* specification. Following a description of the model, we demonstrate the ability of the euSEM to recover parameters used to create simulated data in two Monte Carlos studies. We next apply the euSEM to empirical data taken from a study which utilized an event-related design. The resulting model is fit to a DCM for comparison.

The euSEM proposed here builds upon the uSEM by accounting for the temporal effects of experimental manipulations on ROI activity. Thus the uSEM works best for block designs and the euSEM excels at modeling effective connectivity mapping for event-related designs. For this reason, the hemodynamic response function (HRF) can be incorporated with the euSEM by convolving the vector of onsets of the input with a response function which matches the temporal reaction seen in ROIs (see Friston and Stephan, 2007; Sarty, 2007). This is not possible with the uSEM, which is optimal for block designs. Fig. 1 depicts a decision tree that for modeling effective connectivity models within the general linear model framework which highlights the advances the euSEM makes upon previous models. Furthermore, the euSEM estimates bilinear (or modulating) effects, representing the influence that experimental manipulations has on couplings among ROIs, much like the DCM (see Table 1 for a comparison of the euSEM and DCM). After considering all modeling techniques to date, the euSEM emerges as the only approach that directly estimates the effect of stimuli on brain activity while accounting for both lagged and contemporaneous coupling effects among ROIs.

Estimating modulating influences that experimental manipulations have on couplings attends to a core question in fMRI research: how does brain functioning change when presented with specific stimuli? With bilinear approaches researchers may identify how couplings between ROIs change during stimulation. As mentioned above, a final euSEM model may be derived in an entirely data-driven manner. The euSEM can also be conducted as a confirmatory model if theoretical directions exist. Indeed, the euSEM as implemented in LISREL allows the researcher to constrain some couplings to zero, or require that some couplings be estimated, while exploring additional couplings in a data-driven manner. A final added benefit of the euSEM is that lagged relationships among ROIs and external input are taken into account in a stochastic model.

Formal specification of the euSEM

The following discrete-time bilinear linear system was adapted from Fnaiech and Ljung (1987) and Mathews and Sicuranza (2000). For continuity, the notation used by Kim et al. (2007) was retained for the present model:

$$\eta_t = \underbrace{A\eta_t}_{\text{Cont.}} + \underbrace{\sum_{i=1}^{q} \phi i \eta_{t-i}}_{\text{Lagged}} + \underbrace{\sum_{j=0}^{k} \gamma_j u_{t-j}}_{\text{Input}} + \underbrace{\sum_{i=1}^{s}\sum_{j=i}^{r} \tau_{ij}\eta_{t-i}u_{t-j}}_{\text{Modulating}} + \zeta_t$$

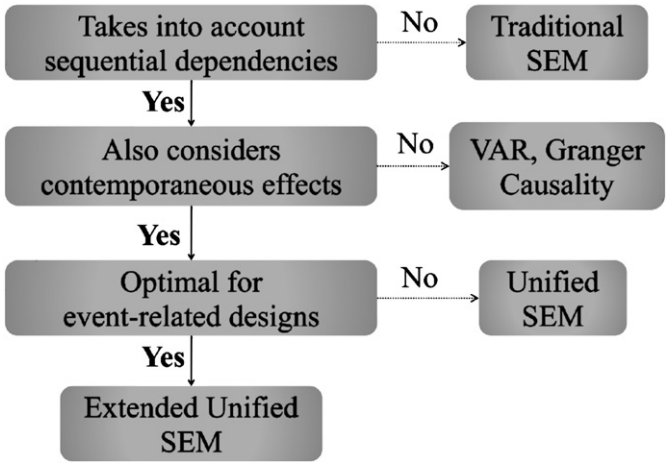

Fig. 1. Decision tree for effective connectivity analysis.

Table 1
Comparison of dynamic causal modeling (DCM) and extended unified structural equation modeling (euSEM).

DCM	euSEM
Currently deterministic	Stochastic
Confirmatory	Exploratory or confirmatory
Bayesian estimation	Maximum likelihood estimation
Models instantaneous change (continuous)	Models contemporaneous and lagged effects (discrete)
Models external input effects and bilinear effects of input and ROI activity	Models external input effects and bilinear effects of input and ROI activity

where η indicates the ROI time series, $\boldsymbol{u}$ a one-vector input series (which may be expanded to include more inputs) convolved with a hemodynamic response function (see Sarty, 2007), A the contemporaneous relations among ROIs, Φ the lagged associations, γ input effects, τ the bilinear associations, and ζ error assumed to be a white noise process. For practical purposes, the equation can be truncated for a lag of one with one input in the following manner:

$$\eta_t = \underbrace{A\eta_t}_{\text{Cont.}} + \underbrace{\phi_1\eta_{t-1}}_{\text{Lagged}} + \underbrace{\gamma_0 u_t + \gamma_1 u_{t-1}}_{\text{Input}} + \underbrace{\tau_{11}\eta_{t-1}u_{t-1}}_{\text{Modulating}} + \zeta_t.$$

Diagnostics in the form of residual analysis may be used to identify if more lags should be considered. Residuals should demonstrate a white noise process when looking at autocorrelations (Lütkepohl, 2005). If a white noise process is not evident, the residuals may be treated to further analysis to identify which variables should have lags of greater order.

Model estimation begins by creating a block Toeplitz matrix of the relations among ROIs, input, and the multiplication of ROI and input activity at time minus one and at time. This approach enables estimates of AR processes that asymptotically approach true maximum likelihood estimates (Hamaker, Dolan, & Molenaar, 2002) and thus may be considered quasi-likelihood (Heyde, 1997). We then select those variables of interest to predict the ROI series at time: ROIs at time minus one (η_{t-1}), ROIs at time (η_t), input at time minus one ($\boldsymbol{u}_{t-1}$) and time ($\boldsymbol{u}_t$), and the dot product of ROI activity and input at time minus one ($\eta_{t-1}\,\boldsymbol{u}_{t-1}$). The beta matrix to be estimated follows the pattern in Table 2. Only parameters that predict ROI activity at time may be freed (either using the automatic search or *a priori* theory) and all others remain fixed. The relations not considered by the beta matrix are modeled as correlations in the psi matrix. By capitalizing on the analytic equivalence between SEM and the state-space framework (Chow, Ho, Hamaker, & Dolan, 2010), the euSEM may be fit within a familiar regression framework.

The euSEM may be estimated by using an automatic search procedure to help identify the optimal model or by selecting the parameters of theoretical interest to apply a confirmatory test. For the automatic search procedure, LISREL first estimates an empty model and utilizes Lagrange multiplier tests (LMTs) to search for the parameter that, if estimated, would best improve overall model fit (for details, see Gates et al., 2010). Only parameters relating to the A, $\boldsymbol{\gamma}$, Φ, and τ matrices are considered in the search procedure for euSEM. In the next iteration, the program frees this parameter and re-estimates the model. The procedure continues until no one parameter would improve the overall fit by the significance level set by the researcher.

Structural identifiability, which is necessary to obtain unique parameter estimates, can be established in the automatic search described above in the following practical way. If a convergent solution is obtained in the automatic search based on the quasi-likelihood method then structural identifiability is almost always guaranteed. In the absence of structural identifiability, the LMT, which

Table 2
Schemata of the beta matrix for four regions and one input estimated using quasi-maximum likelihood implemented in LISREL. "1"s denote parameters that may be set free in accordance to euSEM specifications.

	ROI 1 (t-1)	ROI 2 (t-1)	ROI 3 (t-1)	ROI 4 (t-1)	ROI 1 (t)	ROI 2 (t)	ROI 3 (t)	ROI 4 (t)	INPUT (t-1)	INPUT (t)	ROI 1* INPUT (t-1)	ROI 2 * INPUT (t-1)	ROI 3 * (t-1)	ROI 4 * INPUT (t-1)
ROI 1 (t-1)	0	0	0	0	0	0	0	0	0	0	0	0	0	0
ROI 2 (t-1)	0	0	0	0	0	0	0	0	0	0	0	0	0	0
ROI 3 (t-1)	0	0	0	0	0	0	0	0	0	0	0	0	0	0
ROI 4 (t-1)	0	0	0	0	0	0	0	0	0	0	0	0	0	0
ROI 1 (t)	1	1	1	1	1	1	1	1	1	1	1	1	1	1
ROI 2 (t)	1	1	1	1	1	1	1	1	1	1	1	1	1	1
ROI 3 (t)	1	1	1	1	1	1	1	1	1	1	1	1	1	1
ROI 4 (t)	1	1	1	1	1	1	1	1	1	1	1	1	1	1
INPUT (t-1)	0	0	0	0	0	0	0	0	0	0	0	0	0	0
INPUT (t)	0	0	0	0	0	0	0	0	0	0	0	0	0	0
ROI 1* INPUT (t-1)	0	0	0	0	0	0	0	0	0	0	0	0	0	0
ROI 2 * INPUT (t-1)	0	0	0	0	0	0	0	0	0	0	0	0	0	0
ROI 3 * INPUT (t-1)	0	0	0	0	0	0	0	0	0	0	0	0	0	0
ROI 4 * INPUT (t-1)	0	0	0	0	0	0	0	0	0	0	0	0	0	0

depends upon the Hessian of the likelihood function, would not exist. Because in the quasi-likelihood approach the euSEM is fit to the covariance matrix at a finite number of lags, standard identifiability theory for SEMs can be applied at a more theoretical level. This amounts to determining alpha-numerically the dimension of the null space of the Jacobian of the log-likelihood function with respect to the parameters (Bekker et al., 1994). The euSEM constitutes a subset of a class of recursive polynomial systems (Mathews and Sicuranza, 2000). The stability of the standard model for bounded input $u(t)$ depends on the absolute values of the roots of $(I_p - (I_p - A)^{-1}\Phi_1)$ being smaller than 1, where I_p is the (p,p)-dimensional identity matrix. (for the case of arbitrary orders q, k, s, and r, see Mathews and Sicuranza, 2000, pp. 310–312,).

Application

Monte Carlo simulations

Two sets of simulated data, one with 200 time points and the second with 1,000 time points, were created using the parameters in Table 3. For both sets model errors were generated to be white noise N (0,1) and the input series were generated such that at each time, there was a .3 probability of the event occurring independent of other events. The input series were then convolved with a gamma function to model the hemodynamic response (Sarty, 2007). Table 3 displays the average parameter estimates, standard errors (both analytical averages and empirical estimates), and fit statistics after 100 replications for each length of time series. The procedure successfully identified the correct models as the estimated parameters did not differ significantly from the original parameters used to create the data.

Further support for the appropriateness of the extended unified SEM comes from the excellent model fits obtained in the majority of the replications. With 35 degrees of freedom, chi-square values of less than or equal to 49.8 and 57.3 at a significance levels of $p = .05$ and $p = .01$, respectively, suggest an acceptable model fit. Eighty-five percent of the models estimate for both the NT = 200 and NT = 1000 series were appropriate model fits according to the .05 level criteria, and 96% of the models were appropriate at the .01 level. The chi-square test thus seems too conservative as more models were found to be poor fits than expected by chance. Therefore, four commonly used alternative fit indices were examined. First, the Standardized RMR assesses goodness-of-fit via the mean standardized residuals. The second, root mean square error of approximation (RMSEA), is an absolute measure of fit that estimates the error of approximation per degree of freedom. For these first two indices values under .05 suggests an excellent fit. Working under the assumption that the fit function of the estimated model is chi-square distributed, the Non-Normed Fit Index (NNFI) penalizes the model for each parameter added. Finally, the comparative fit index assumes a noncentral chi-square distribution (Hu & Bentler, 1998). The latter two indices penalize the models for each parameter added and values of .95 and above indicate an excelled model fit (Kenny and McCoach, 2003; Schermelleh-Engel et al., 2003). According to these four indices all of the estimated models demonstrated excellent fits.

Empirical data example: rapid processing task

Procedure

Data were acquired as part of a larger study examining deficits in processing speed for individuals with multiple sclerosis. The present data were extracted from one healthy female participant aged 49 years and Caucasian. Details of the study have been published elsewhere (Genova et al., 2009; Hillary, et al., 2010). Briefly, the study used the modified Digit Symbol Substitution Task (Rypma et al., 2006; Smith, 1982) to assess processing speed. The subjects were presented with two boxes: one reference box containing paired numbers and symbols and one probe box containing only one pair of a number and symbol. Respondents were given up to 6 seconds to indicate whether the probe appeared in the reference box. There were three trials each lasting 7 minutes and 48 seconds and containing 225 TRs. Following a practice period, 153 events were presented to the subject during MRI acquisition.

MRI data processing

Neuroimaging was performed at the University of Medicine and Dentistry of New Jersey on a Siemens Allegra 3 T MRI. Sagittal T1-weighted scout images were obtained for localization. Whole brain axial T1-weighted conventional spin-echo images (in-plane resolution = 0.859 mm2) for anatomic underlays (TR/TE = 450/14 ms, contiguous 5 mm, 256 × 256 matrix, FOV = 24 cm, NEX = 1) were then obtained. Functional imaging consisted of multislice gradient echo, T2*-weighted images acquired with echoplanar imaging (EPI) methods (TE = 60 ms; TR = 2000 ms; FOV = 24 cm; flip angle = 90°; slice thickness = 5 mm contiguous), yielding a 64 × 64 matrix with an in-plane resolution of 3.75 mm2.

Analysis of MRI data

Image processing and initial statistical analysis were conducted with Statistical Parameter Mapping (Friston, et al., 1995) version 5

Table 3
Results from two Monte Carlos simulation studies with number of time points (NT) equal to 200 and 1000. Numbers in parentheses below the average parameter estimates are the average standard error on the left of the dash and the empirical standard error on the right. "–" denotes that the parameter was not estimated. NT = number of time points in simulation.

	Parameters for Simulation				**Estimated Parameters** (NT=200)				**Estimated Parameters** (NT=1000)			
Φ	0.40	0	0	0	.39 (.06/.06)	--	--	--	0.40 (.03/.03)	--	--	--
	0	0.40	0	0	--	.39 (.06/.05)	--	--	--	0.40 (.03/.02)	--	--
	0	0	0.40	0	--	--	.39 (.06/.06)	--	--	--	0.40 (.03/.03)	--
	0	0	0.30	0.40	--	--	.30 (.06/.06)	.39 (.05/.05)	--	--	0.30 (.03/.03)	0.40 (.03/.03)
A	0	0	0	0	--	--	--	--	--	--	--	--
	0	0	0.40	0	--	--	.41 (.06/.06)	--	--	--	.40 (.03/.03)	--
	0.40	0	0	0	0.38 (.06/.08)	--	--	--	.38 (.03/.03)	--	--	--
	0	0	0	0	--	--	--	--	--	--	--	--
γ_0	0.20	0	0	0	.20 (.07/.07)	--	--	--	.21 (.03/.03)	--	--	--
γ_1	0	0.30	0	–0.30	--	.32 (.07/.08)	--	-.31 (.08/.08)	--	.30 (.03/.04)	--	-.30 (.03/.03)
τ	0	0	0	0	--	--	--	--	--	--	--	--
	0	0	0	0	--	--	--	--	--	--	--	--
	0	0	0	0	--	--	--	--	--	--	--	--
	0	0	0.50	0	--	--	.49 (.06/.06)	--	--	--	.50 (.03/.02)	--

(http://www.fil.ion.ucl.ac.uk/spm5). To control for initial signal instability, the first nine volumes were removed from analyses. Preprocessing steps included realignment of functional data to the first functional image using affine transformation (Ashburner et al., 1997; Friston et al., 1995). Images were coregistered to the TI MPRAGE and all data were normalized using a standardized T1 template from the Montreal Neurological Institute, using a 12-parameter affine approach and bilinear interpolation. Then, normalized time series data were smoothed with a Gaussian kernel of $8\times8\times10\text{mm}^3$. Time series for the right and left prefrontal cortex (RPFC and LPFC) and the right and left cerebellum (RCB and LCB) were selected by obtaining the first principal component scores in these regions. The first and last data points of the time series were shed due to extremely large values.

Results

The model of couplings among ROIs was selected by employing the automatic search procedure. An alternative and feasible approach would be to identify couplings among ROIs and the experimental manipulation *a priori* and use the automatic search procedure to investigate other paths which may improve the model. For the present purposes, a model was selected based predominantly on the alternative indices previously discussed which have demonstrated reliability in simulation studies (Brown, 2006): RMSEA, Standardized RMR, NNFI, and CFI. Then, we looked at later iterations to identify modulating terms to add to this underlying structural model. The rationale for this approach comes from the insight that it takes substantial power to detect multiplicative terms (Cronbach, 1987). Thus, modulating effects, which are what researchers are interested in exploring, may not surface as early in the iterative procedure as main effects. The selected model containing the underlying coupling parameters had a chi-square of 118.46 (df = 38) but demonstrated a good fit by indices not as sensitive to sample size: RMSEA = .056, standardized RMR = .033, NNFI = .93, and CFI = .97. A modulating effect surfaced five iterations later which was significant. When this effect was added to the model with coupling parameters, the final model again had an excellent fit: 112.05 (df = 37), RMSEA = .056, standardized RMR = .029, NNFI = .94, and CFI = .97 (see Fig. 2). The residual process was investigated by estimating the autocorrelation function (ACF) for the prediction of ROI activity (see Fig. 2). The residuals demonstrate a white noise process, suggesting that a lag of one is sufficient to predict ROI activity in these data.

The influence of the stimuli on ROI activity appears to be predominantly direct for this individual (see Fig. 3). For instance, direct effects for the stimuli on the RPFC and LCB exist. The only modulating effect was seen for RPFC: in the presence of the stimuli, the autoregressive effect for this ROI becomes negative. This suggests

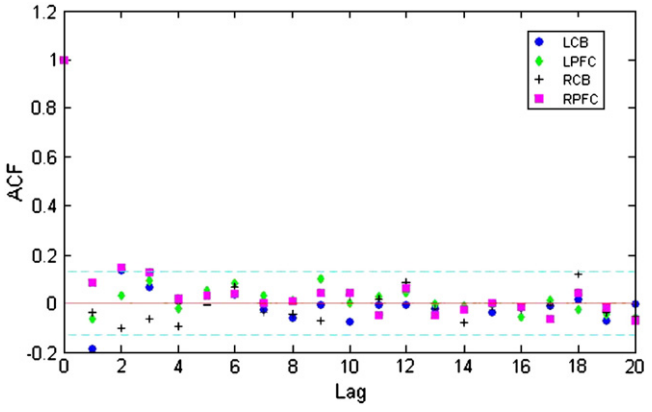

Fig. 2. Autocorrelation function (ACF) of residuals obtained from final model. Dotted sea green lines indicate confidence intervals at the Bonferroni-corrected level.

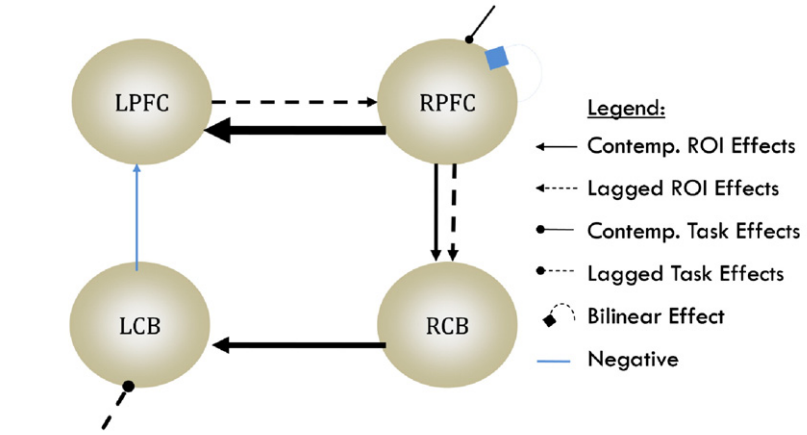

Lagged Effects

	Φ				γ
	LCB(t-1)	LPFC(t-1)	RCB(t-1)	RPFC(t-1)	Task(t-1)
LCB(t)	--	--	--	--	.16(.03)
LPFC(t)	--	--	--	--	--
RCB(t)	--	--	--	.27(.04)	--
RPFC(t)	--	.25(.04)	--	--	--

Contemporaneous Effects

	A				γ
	LCB(t)	LPFC(t)	RCB(t)	RPFC(t)	Task(t)
LCB(t)	--	--	.42(.03)	--	--
LPFC(t)	-.15(.03)	--	--	.65 (.03)	--
RCB(t)	--	--	--	.27 (.04)	--
RPFC(t)	--	--	--	--	.29(.04)

Lagged Bilinear Effects

	τ			
	LCB*Task(t-1)	LPFC*Task(t-1)	RCB*Task(t-1)	RPFC*Task(t-1)
LCB(t)	--	--	--	--
LPFC(t)	--	--	--	--
RCB(t)	--	--	--	--
RPFC(t)	--	--	--	-.09(03)

Fig. 3. Extended unified SEM results for empirical data. Contemp. = Contemporaneous. Numbers in parentheses are standard errors of the parameter estimates. "–" denotes that the parameter was not estimated. Thickness of lines corresponds with magnitude of relationship.

that a system occurs by which BOLD activity increases when the previous scan's activity was low, and decreases when it was previously high. Thus, one might interpret this as the ROI modulating itself or damping activity in the presence of excitatory influence. The direct contemporaneous relation between the stimuli and RPFC is positive, suggesting that when a stimulus is shown the RPFC has increased activity. These relationships among the stimuli and RPFC appear to be particularly important since the RPFC exerts influence on RCB and LPFC directly and the LCB indirectly via the RCB. Furthermore, although the LPFC and RCB demonstrated significant BOLD signal changes in the presence of the experiment manipulation when tested using the general linear model, the connectivity map evidenced no direct influences of the stimuli on activation. The rises in activity associated with the stimuli are best explained by its relationship with the other ROIs. The stimuli indirectly influence variation in the LPFC via the lagged and contemporaneous relationship they have with the RPFC and LCB, and similarly influenced RCB via its relationship with RPFC.

Comparing extended unified SEMs with dynamic causal models

The data-driven euSEM obtained via the automatic search procedure was then subjected to confirmatory dynamic causal modeling. This exercise demonstrates the utility of using the automatic search procedure to first identify a plausible model and subsequently test the model using the DCM for researchers wishing to use the DCM approach. As a reminder, a major substantive difference between the extended unified SEM and the DCM is that the DCM incorporates a neural-hemodynamic model whereas the extended

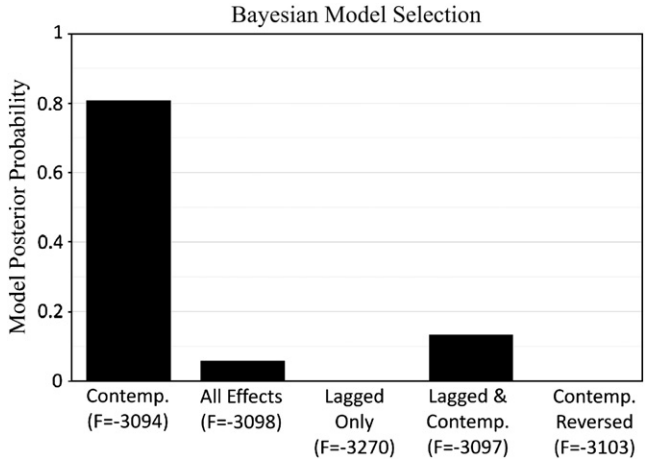

Fig. 4. DCM model selection figures. The models with higher posterior probabilities are better fitting. Full model descriptions may be found in the text.

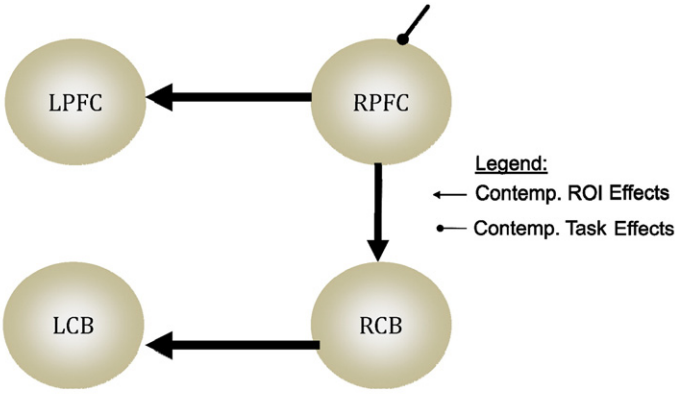

DCM Results

	LCB	LPFC	RCB	RPFC	Task	LCB* Task	LPFC* Task	RCB* Task	RPFC* Task
LCB	--	--	0.65 (1.00)	--	--	--	--	--	--
LPFC	0.06 (0.65)	--	--	0.42 (1.00)	--	--	--	--	--
RCB	--	--	--	0.52 (1.00)	--	--	--	--	--
RPFC	--	--	--	--	0.28 (1.00)	--	--	--	0.01 (0.52)

Fig. 5. Estimates from dynamic causal model. Contemp. = Contemporaneous. "–" indicates no parameter was estimated. For ease in comparison with the euSEM, only parameter estimates with posterior probabilities greater than .90 were retained in the figure.

unified SEM models the BOLD response without making assumptions regarding the neural-hemodynamic process. However, the euSEM can be used for confirmatory models for researchers wishing to remain agnostic about the neural-hemodynamic relationship.

By modeling change occurring at an infinitesimal time, the DCM model most comparable to the euSEM would presumably be one that considers only contemporaneous effects and not the lagged effects, which occur at the time span of the scans. Still, we wanted to test whether the best DCM model obtained was in fact the one which modeled the contemporaneous couplings among ROIs. Thus, we specified four DCM models to test. The first contained only the contemporaneous relations found in the euSEM (allowing for the lagged modulating term), the second contained the contemporaneous plus lagged effects and all inputs, the third the lagged relations, and the fourth lagged and contemporaneous. The model containing only the contemporaneous couplings and inputs plus the modulated lagged effect from the euSEM was the best model fit. To ensure that this model was not considered the best solely as a function of the number of parameters included, we also reversed the contemporaneous model so that the directed arrows went the opposite direction. Still, the model with only the contemporaneous and modulating relations found in the euSEM was best (see Fig. 4). Fig. 5 displays the diagram and parameter estimations for the selected DCM. Comparing the contemporaneous and modulating effects found in the euSEM with those found in the DCM reveals a few differences. For one, the contemporaneous effect for LCB regressed on LPFC, while significant in the euSEM, was found to be below the suggested criteria of 90% posterior probability for retention in the DCM (Stephan et al., 2010). The modulating effect for the autoregression of RPFC was similarly negligible in the DCM despite being significant in the extended unified SEM.

Discussion

Functional MRI data have the potential to offer rich insight into the orchestration of brain activity. Much of the work to date has focused on identifying which areas of the brain become active when presented with specific stimuli or task demands. Having identified ROIs associated with specific mental processes, researchers now wish to answer more complicated questions that take into account the temporal ordering of activity. Connectivity modeling offers critical additional information about neural systems for researchers in a broad range of substantive backgrounds who seek to understand the mechanisms by which normal and atypical functioning occur. The euSEM presented in this paper offers a practical and complete method for examining relations among ROIs while including information about experimental manipulations, thus offering several important advantages for connectivity modeling in fMRI time series data.

The greatest advancement that the euSEM offers over current connectivity models is the inclusion of direct and modulating effects of external input on ROI activity. Indeed, although most research examining brain function includes external input, there remain important limitations with respect to how inputs can be modeled. To date, documenting the influence of external input on covariance between ROIs requires separate connectivity maps for each "on-task" epoch. This necessitates the use of block designs not out of a substantive interest or theoretical view that the brain functions in discrete states but due to methodological limitations. The euSEM provides an integrated framework for examining ROI behavior within distributed neural networks and, importantly, permits inferences regarding how stimuli affect ROI covariance at the level of individual events.

Given that neural connectivity modeling in systems neuroscience remains in its infancy data-driven, exploratory approaches to examine covariance in ROIs may be particularly advantageous. In this way, the euSEM again offers a clear advantage over other approaches. Following from the method outlined in Gates et al. (2010) we present here confirmatory models acquired from an entirely data-driven procedure on previously specified ROIs. The exploratory method considers all possible relations among ROIs (including lagged effects) as well as the lagged modulating effect that external input may have on the connection before selecting the next parameter to free for estimation. Such an approach is ideal for theory development. A second way in which researchers may use the exploratory procedure would be to directly compare the best model derived via a data-driven approach with a hypothesized connectivity map. Confirmation that a proposed model does not significantly differ from an entirely data-driven model would strongly bolster the findings. Finally, the data-

driven model may help research that has support for hypothetical connections identify additional couplings among ROIs that, while not included in their theory, improves the overall model fit and insight into brain processes.

The sole alternate bilinear method for modeling event-related designs is the DCM. As demonstrated here, the euSEM may be used in tandem with the DCM by utilizing the automatic search procedure to arrive at a confirmatory model which may inform DCM models. However, as demonstrated in the present paper, the two approaches may yield different results. This is partly because integral to the DCM is the inclusion of information about the neuronal-hemodynamic relationship whereas the euSEM does not make any assumptions regarding the relationship between the vascular response obtained from the BOLD signal and neural activity. For this reason, the extended unified SEM may be an appropriate alternative for researchers wishing to remain agnostic regarding this relationship.

The final benefit offered by the euSEM is the simultaneous estimation of lagged and contemporaneous relationships. The euSEM results likely differ from the DCM because the DCM does not directly model relations occurring at the lag time associated with scans. Prior research has demonstrated the biases introduced when both sources of variation are not considered (Gates et al., 2010; Kim et al, 2007). Still, researchers must be careful not to assign causality solely based on establishing temporal ordering of BOLD activity among ROIs because delays in BOLD response to stimuli vary across regions and subjects (Lindquist, 2008; Robinson et al., 2010). The relationship between the BOLD signal and neuronal activity remains poorly understood (de Marco et al., 2009) and correlated changes in BOLD responses may be artifacts of differences in ROIs' physiology. Indeed, evidence suggests that the delay between neural activity and vascular response differ by regions (Vazquez et al., 2006). Thus, one must be careful when suggesting causality whenever using BOLD data. Future research needs to continue examining how to best take into account differences in BOLD responses when modeling connectivity patterns.

Acknowledgments

This work was supported by a National Science Foundation grant (0852147).

References

Ashburner, J., Neelin, P., Collins, D.L., Evans, A., Friston, K., 1997. Incorporating prior knowledge into image registration. Neuroimage 6 (4), 344–352.
Bekker, P.A., Merckens, A., Wansbeek, T.J., 1994. Identification, equivalent models, and computer algebra. Academic Press, Boston.
Brown, T. A. 2006. Confirmatory Factor Analysis for Applied Research. Gilford Press. New York.
Chow, S.M., Ho, M.R., Hamaker, E.L., Dolan, C.V., 2010. Equivalence and differences between structural equation modeling and state-space modeling techniques. Struct. Equ. Model.: Multi. J. 17, 303–332.
Cronbach, L.J., 1987. Statistical tests for moderator variables: flaws in analyses recently proposed. Psychol. Bull. 102, 414–417.
de Marco, G., Devauchelle, B., Berquin, P., 2009. Brain functioning modeling, what do we measure with fMRI data? Neurosci. Res. 64, 12–19.
Fnaiech, F., Ljung, L., 1987. Recursive identification of bilinear systems. Int. J. Control 45, 453–470.
Friston, K.J., 2007. Dynamic causal modeling. In: Friston, K.J., Ashburner, J.T., Kiebel, S.J., Nichols, T.E., Penny, W.D. (Eds.), Statistical parametric mapping: the analysis of functional brain images. Amsterdam: Academic Press, pp. 541–560.
Friston, K.J., Stephan, K., 2007. Modeling brain responses. In: Friston, K.J., Ashburner, J.T., Kiebel, S.J., Nichols, T.E., Penny, W.D. (Eds.), Statistical parametric mapping: the analysis of functional brain images. Academic Press, Amsterdam, pp. 32–45.
Friston, K.J., Holmes, A.P., Poline, J.B., Grasby, P.J., Williams, S.C., Frackowiak, R.S., Turner, R., 1995. Analysis of fMRI time-series revisited. Neuroimage 2, 45–53.
Friston, K.J., Buechel, C., Fink, G.R., Morris, J., Rolls, E., Dolan, R.J., 1997. Psychophysiological and modulatory interactions in neuroimaging. Neuroimage 6, 218–229.
Gates, K.M., Molenaar, P.C.M., Hillary, F., Ram., N., & Rovine, M., 2010. Automatic search for fMRI connectivity mapping: An alternative to Granger causality testing using formal equivalences between SEM path modeling, VAR, and unified SEM. NeuroImage 53, 1118–1125.
Genova, H.M., Hillary, F.G., Wylie, G., Rypma, B., Deluca, J., 2009. Examination of processing speed deficits in multiple sclerosis using functional magnetic resonance imaging. J. Int. Neuropsychol. Soc. 15, 383–393.
Goebel, R., Roebroeck, A., Kim, D.S., Formisano, E., 2003. Investigating directed cortical interactions in time-resolved fMRI data using vector autoregressive modeling and Granger causality mapping. Magn. Reson. Imaging 21, 1251–1261.
Hamaker, E.L., Dolan, C.V., Molenaar, P.C.M., 2002. On the nature of SEM estimates of ARMA parameters. Struct. Equ. Model. 9, 347–368.
Harrison, L., Stephen, K., Friston, K., 2007. Effective connectivity. In: Friston, K.J., Ashburner, J.T., Kiebel, S.J., Nichols, T.E., Penny, W.D. (Eds.), Statistical parametric mapping: the analysis of functional brain images. Academic Press, Amsterdam, pp. 508–521.
Heyde, C.C., 1997. Quasi-likelihood and its application: a general approach to optimal parameter estimation. Springer, New York.
Hillary, F.G., Genova, H.M., Medaglia, J.M., Fitzpatrick, N.M., Chiou, K.S., Wardecker, B.M., DeLuca, J., 2010. Speed of information processing deficits in traumatic brain injury: is less brain more? Brain Imaging Behav. 4, 141–154.
Hu, L., Bentler, P.M. 1998. Fit indices in covariance structure modeling: sensitivity to underparameterized model misspecification. Psychol. Methods 3, 424–453.
Kenny, D.A., McCoach, D.B., 2003. Effect of the number of variables on measures fit in structural equation modeling. Struct. Equ. Model.: Multi. J. 10, 333–351.
Kim, J., Zhu, W., Chang, L., Bentler, P.M., Ernst, T., 2007. Unified structural equation modeling approach for the analysis of multisubject, multivariate functional MRI data. Hum. Brain Mapp. 28, 85–93.
Lindquist, M.A., 2008. The statistical analysis of fMRI data. Stat. Sci. 23, 439–464.
Lütkepohl, Helmut, 2005. New introduction to multiple time series analysis. Springer, Berlin.
Mathews, V.J., Sicuranza, G.L., 2000. Polynomial signal processing. John Wiley & Sons, Chichester, England.
McIntosh, A.R., Gonzalez-Lima, F., 1994. Structural equation modeling and its application to network analysis in functional brain imaging. Hum. Brain Mapp. 2, 2–22.
Raichle, M.E., Snyder, A.Z., 2007. A default mode of brain function: a brief history of an evolving idea. Neuroimage 37, 1083–1090.
Robinson, L.F., Wager, T., Lindquist, M., 2010. Change point estimation in multi-subject fMRI studies. Neuroimage 49, 1581–1592.
Rypma, B., Berger, J.S., Prabhakaran, V., Bly, B.M., Kimberg, D.Y., Biswal, B.B., D'Esposito, M., 2006. Neural correlates of cognitive efficiency. Neuroimage 33, 969–979.
Sarty, G.E., 2007. Computational brain activity maps from fMRI time-series images. Cambridge University Press, New York.
Schermelleh-Engel, K., Moosbrugger, H., Müller, H., 2003. Evaluating the fit of structural equation models: Descriptive goodness-of-fit measures. Methods Psychol. Res. Online 8, 23–74.
Smith, A., 1982. Symbol Digits Modalities Test. Western Psychological Services, Los Angeles, CA.
Sporns, O., Chialvo, D.R., Kaiser, M., Hilgetag, C.C., 2004. Organization, development, and function of complex brain networks. Trends Cogn. Sci. 8, 418–426.
Stephan, K.E., Penny, W.D., Moran, R.J., den Ouden, H.E.M., Daunizeau, J., Friston, K.J., 2010. Ten simple rules for dynamic causal modeling. Neuroimage 49, 3099–3109.
Tononi, G., Edelman, G.M., Sporns, O., 1998. Complexity and coherency: integrating information in the brain. Trends Cogn. Sci. 2, 474–484.
Vazquez, A.L., Cohen, E.R., Gulani, V., Hernandez-Garcia, L., Zheng, Y., Lee, G.R., Kim, S.G., Grotberg, J.B., Noll, D.C., 2006. Vascular dynamics and bold fMRI: Cbf level effects and analysis considerations. Neuroimage 32, 1642–1655.